Materials and Design 31 (2010) 1200–1207

Contents lists available at ScienceDirect

Materials and Design

journal homepage: www.elsevier.com/locate/matdes

Effect of matrix alloy and influence of SiC particle on the sliding wear characteristics of aluminium alloy composites

R.N. Rao [a,*], S. Das [b]

[a] Department of Mechanical Engineering, National Institute of Technology, Warangal 506 021, India
[b] Advanced Materials and Processes Research Institute, Bhopal 462 026, India

ARTICLE INFO

Article history:
Received 20 July 2009
Accepted 17 September 2009
Available online 26 September 2009

Keywords:
Matrix alloy
AA7010
SiC
Wear mechanism
Mechanically mixed layer
Wear resistance

ABSTRACT

This article presents an effect of matrix alloy and influence of SiC particle on the sliding wear characteristics of high strength aluminium alloys AA7010, AA7009 and AA2024, composites was examined under varying applied pressure and a fixed sliding speed of 3.35 m/s. The results revealed that the wear resistance of the composite was noted to be significantly higher than that of the alloy and is suppressed further due to addition of SiC particles. The overall observation among the matrix alloys, AA7010 alloy shows maximum wear resistance than that of the other, and can withstand the seizure pressure up to 2.6 MPa. The wear mechanism was studied through worn surfaces and microscopic examination of the developed wear tracks. The wear mechanism strongly dictated by the formation and stability of oxide layer, mechanically mixed layer (MML) and subsurface deformation and cracking. The overall results indicate that the high strength aluminium alloys and composite could be considered as an excellent material where high strength and wear resistance components are prime importance especially designing for structural applications in aerospace and general engineering sectors.

1. Introduction

Aluminium matrix composites reinforced with hard ceramic particles have emerged as a potential material especially for wear resistant and weight critical applications [1]. Aluminium matrix composites offer superior wear and seizure resistance as compared to the alloy irrespective of applied load and sliding speed. This is primarily due to the fact that the hard dispersoid makes the matrix alloy plastically constrained and improves the high temperature strength of the virgin alloy [2]. Additionally, the hard dispersoids, present on the surface of the composite as protrusions, protect the matrix from the severe contact with the counter surfaces [3,4], and thus resulting in less wear, lower coefficient friction and temperature rise in composite as compared to that in the alloy [5,6]. On the other hand, a few in investigators reported higher values of coefficient of friction of AMCs as compared to the alloy [7–14]. According to these investigators, this may be due to (i) greater depth of penetration of hard dispersoids onto the counter surface and (ii) fracture/fragmentation of the dispersoids, which in due coarse gets entrapped into the contact surface.

Limited attempts have been to examine the effect of matrix alloy on the sliding wear behaviour of aluminium alloy and composites. It was observed that the transition load as well as wear or seizure resistance of pure aluminium could be increased significantly with increase in SiC content [7]. They reported that the transition load for Al, Al–10%SiC and Al–40%SiC are 45, 120 and 240 N respectively. They also tried to correlate transition load with hardness. It is observed by these investigators that even the hardness of other Al alloy is higher than that of composite; the transition load is noted to be less than that of composites. They explained on the basis of different nature of MML in alloy and composites, subsurface cracking and micro structural change. It is reported that the transition load increases with increase in hardness of MML and with decrease in thickness of the MML. The thickness of MML is noted to be maximum at some intermediate load. Sahin and Murphy [15] observed that wear resistance of the alloy improved significantly (2–6 times) depending on applied load by addition of 16% Al_2O_3 fiber, but further increase in fiber content leads only marginal improvement in wear resistance. Improvement in wear resistance with fiber content could be due to (i) reduced depth of subsurface plastic deformation, (ii) stronger surface of MMCs, (iii) embedding of boron particles and fragmented fibers on the MIL and (iv) rotation of wear debris on and between the fibers. This is in good agreement with the observation of Murphy and Arikan [16].

In recent times, attention is being paid to the use of high strength aluminium alloys for structural applications in aerospace

* Corresponding author. Tel.: +91 9490164981; fax: +91 8702459547.
E-mail address: rnraonitw@gmail.com (R.N. Rao).

0261-3069/$ - see front matter © 2009 Elsevier Ltd. All rights reserved.
doi:10.1016/j.matdes.2009.09.032

and general engineering sectors. However, these materials are of poor weldability [17]. Thus, most of these materials are joined either by riveting or bolting, and hence there is a greater possibility of vibration or oscillation in these regions, which in due course might be leading to fretting and sliding type of wear in dry conditions. This demands the need to examine the dry sliding wear characteristics of these alloy systems. However, limited attempt has been made to examine the wear characteristics of 7xxx Al-alloy in as-cast and heat treated condition [7]. Sliding wear characteristics of 7xxx series alloy especially as compared to the 7xxx series-SiC composite is lacking even though they have good potential to be used as airplane structural sheets and armour materials.

In view of the above, in the present study, effect of matrix alloy and sliding wear characteristics of high strength aluminium alloys AA7010, AA7009 and AA2024 silicon carbide particle composite was examined under varying applied pressures at a fixed sliding speed of 3.35 m/s. These alloys and their composites are processed in similar manner in order to compare their effect on the tribological behaviour under varying experimental condition. The trend of variation in several tribological parameters like wear rate, seizure pressure, frictional heating and coefficient of friction the selected alloy and composite systems noted to be almost same. Hence for better comparison between the different alloy and composite systems systematically, selected results are projected.

2. Methods

2.1. Material preparation

Al–Zn–Mg–Cu, Al–Zn–Mg and Al–Mg–Cu alloys, SiC particle composite have been used for present study and the chemical compositions of the matrix alloys are shown in Table 1. The composite was synthesized through solidification processing (stir-casting) route using SiC particle of size range 20–40 μm as reinforcement. The process involved melting the alloy, incorporation of preheated SiC particles in the melt through mechanically stirring, casting of the composite melt in the preheated permanent cast iron mould. The alloy melt was also cast in same permanent cast iron die in the form of cylinder of 200 mm in length and 16 mm in diameter.

2.2. Microscopy

For micro structural studies of AA7010 aluminium alloy and silicon carbide particle reinforced Al composites in as cast conditions, samples of dimensions 20 mm diameter and 15 mm thick were cut and cold mounted. The specimens were mechanically polished using standard metallographic practices and etched with Kellor's reagent (1% HF, 1.5% HCl, 2.5% HNO_3 and remaining water) prior to their micro structural examination by optical (Leitz Metalloplan) and scanning electron microscopy (Model: JEOL, JSM-5600). The samples were sputtered with gold prior to scanning electron microscopic examination. The worn surfaces and subsurface regions after sliding wear tests were also examined by scanning electron microscope.

Table 1
Chemical compositions of aluminium alloys (in wt.%).

Element (wt.%)	AA7010	AA7009	AA2024
Fe	0.27	0.29	0.49
Cu	1.28	0.01	4.46
Mn	–	–	0.59
Mg	1.14	1.63	1.86
Zn	5.307	5.855	0.034
Al	Balance	Balance	Balance

2.3. Sliding wear tests

Sliding wear tests were conducted in pin-on-disc wear testing apparatus (model: TR20-LE, Wear and Friction Monitor, Ducom Make, Bangalore, India) under varying applied pressures at a fixed sliding speed of 3.35 m/s against EN32 steel disc of hardness 500 HV. The pin samples were 27 mm in length and 8 mm in diameter. The surfaces of the pin sample and the steel disc were ground using emery paper prior to each test. In ordered to ensure effective contact of fresh surface with the steel disc, the fresh samples were subjected to sliding on emery paper of 240 grit size fixed on the steel disc. During sliding, the load is applied on the specimen through cantilever mechanism and the specimens brought in intimate contact with the rotating disc at a track radius of 100 mm (Fig. 1). The samples were cleaned with acetone and weighed (up to an accuracy of 0.01 mg using microbalance) prior to and after each test. The wear rate was calculated from the weight loss technique and expressed in terms of volume loss per unit sliding distance.

The temperature rise and friction force were recorded from the digital display interfaced with the wear test machine. In order to record the temperature, the bare end of a chromel–alumel thermocouple was inserted into a small drill hole (1.5 mm diameter) in the lateral surface of the specimen, at a distance of 1.5 mm away from the contacting surface. Coefficient of friction was computed from the recorded frictional force and the applied load (i.e. the ratio of frictional force to the applied load). A set of three samples was tested in every experimental condition, and the average along with standard deviation for each set of three tests is measured. The wear tests were conducted either up to a sliding distance of 5000 m or up to the distance at which the material seized, which one occurs earlier. The occurrence of seizure was defined by the generation of abnormal sound and vigorous vibration during the test, and sudden increase in frictional force and temperature rise (because of adhesion between the two contact surfaces under high temperature rise and frictional force). Sticking of material (displaced material from the specimen surface) was also noted on the steel disc by naked eye. The applied load (pressure) and sliding distance are

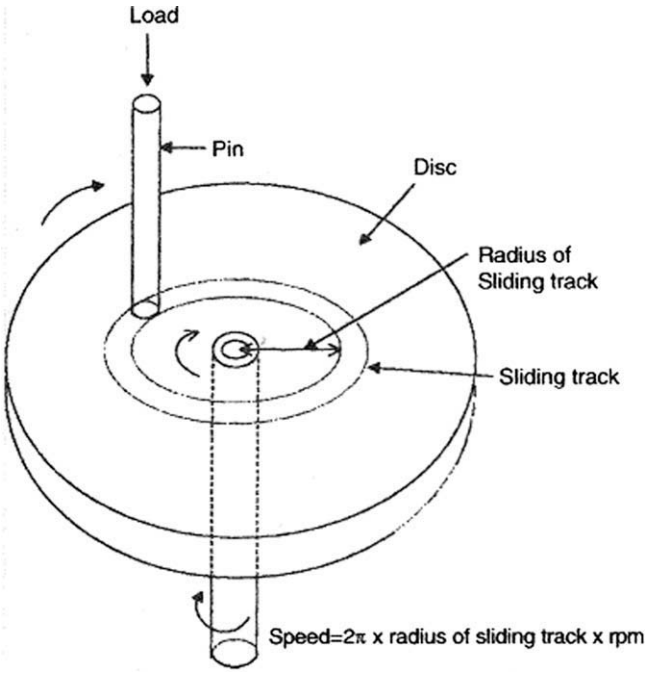

Fig. 1. Schematic diagram of pin-on-disc test set up.

recorded when the specimen gets seized for calculation of seizure pressure, coefficient of friction and wear rate.

3. Results

3.1. Microstructure of aluminium alloy and composites

The microstructure of AA7010 (Al–Zn–Mg–Cu) alloy consists of dendrites of Al and precipitates along the interdendritic regions in Fig. 2a. A higher magnification micrograph clearly shows the Al dendrites (marked A) and the precipitates along the dendrite boundaries (arrow marked) in Fig. 2b. A higher magnification micrograph clearly shows the formation of precipitates found the Al matrix. The morphology of the precipitates varies from equiaxed lamellar. The equiaxed precipitates are of 2–5 μm in size. The lamellar precipitates are usually are of around 10–15 μm in length, and 2–3 μm in width. The micrograph of Al–Zn–Mg–Cu-10 wt.% SiC reinforced composite is shown in Fig. 2c. It clearly shows the uniform distribution of SiC particle in 7010 alloy matrix. Fig. 2d shows the good interface bonding between SiC and matrix.

3.2. Effect of matrix alloy

Composite materials are the mixture of two or more phases in which each of the phase retains their physical, chemical and mechanical characteristics. The properties of composite materials are dictated both by the reinforcing phase (minor phase) and the matrix alloy. Thus the microstructure and chemistry of matrix alloy in composite may considerably influence the mechanical as well as tribological behaviour of the composite material. In order to examine the effect of matrix alloy and tribological behavior of the composites, these alloy systems namely AA7009, AA7010 and AA2024 are used in the present study. These alloys and their composites are processed in similar manner in order to compare their effect on the tribological behaviour under same experimental condition. The trend of variation in several tribological parameters like wear rate, seizure pressure, frictional heating and coefficient of friction the selected alloy and composite systems noted to be almost same. Hence it is found that it is not necessary to project all the results relating to the above mentioned tribological parameters at all experimental conditions. Hence for better comparison between the different alloy and composite systems systematically selected results are projected in this subsection.

3.2.1. Effect of matrix alloy on wear rate

The bar chart of wear rate of different alloys and their composites in as cast conditions at a sliding speed of 3.35 m/s and fixed applied pressure of 1.2 MPa is shown in Fig. 3a. It is evident form this figure that the 2024 alloy system suffers from highest wear rate, where as the 7010 alloy system exhibited least wear rate irrespective of SiC content and processing condition. For example, the wear rate of 7010, 7009 and 2024 alloy are noted to be 2.2, 2.36 and 2.92×10^{-12} m^3/m respectively. In case of 10 wt.% SiC reinforced composite the wear rate for 7010, 7009 and 2024 matrix alloy systems are noted to be 1.78, 1.94 and 2.27×10^{-12} m^3/m respectively. Similarly in case of 25 wt.% SiC reinforced composites, the wear rate of 7010, 7009 and 2024 alloys are noted to be 1.1, 1.35 and 1.63×10^{-12} m^3/m respectively. But matrix alloy and SiC reinforcement play an important role in controlling the wear behaviour.

3.2.2. Effect of matrix alloy on temperature rise

Fig. 3b represents the seizure temperature of different alloy and composites at sliding velocity of 3.35 m/s at a seizure pressure of different alloying systems. It is evident from this figure that irrespective of processing conditions and SiC content, maximum seizure temperature is noted in AA7010 alloy and minimum is noted for 2024 alloy system. But, the seizure temperature increases very marginally with increasing SiC content. For example the seizure temperature of matrix 7010, 7009 and 2024 alloys are noted to be 152, 145, 135 °C respectively. In case of Al–10 wt.% SiC composites, the seizure temperatures for 7010, 7009 and 2024 alloys in as cast condition are noted to be 164, 156 and 151 °C respectively. The seizure temperature is increased with addition of SiC content.

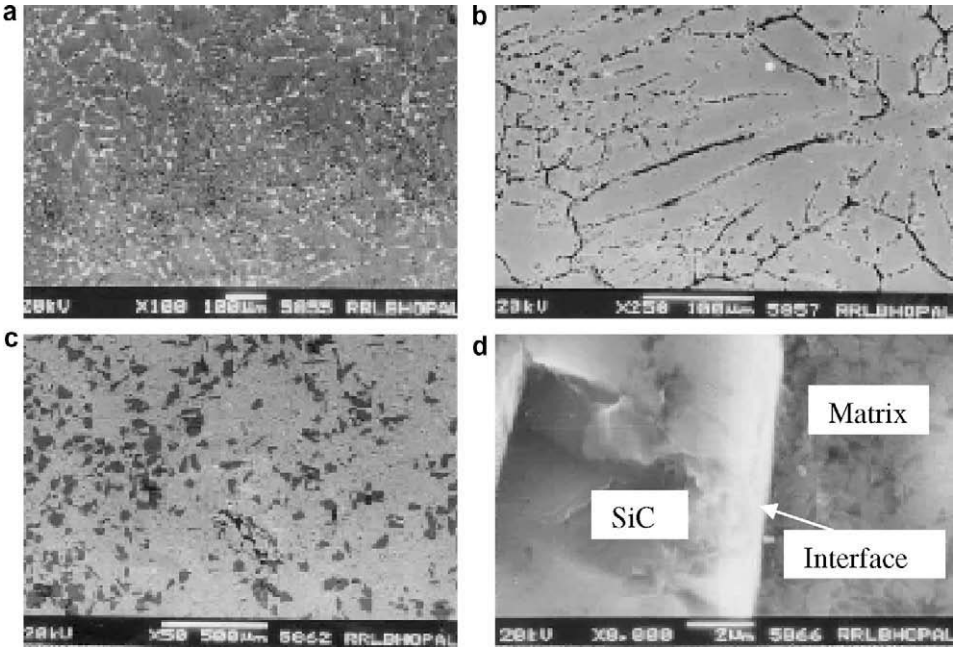

Fig. 2. Microstructure of AA7010 aluminium alloy and composite (a) SEM micrograph of cast alloy, (b) a higher magnification micrograph of as cast alloy, (c) as cast composite showing uniform distribution of SiC particles, and (d) higher magnification micrograph of as cast composite showing good bonding between the matrix and SiC particle.

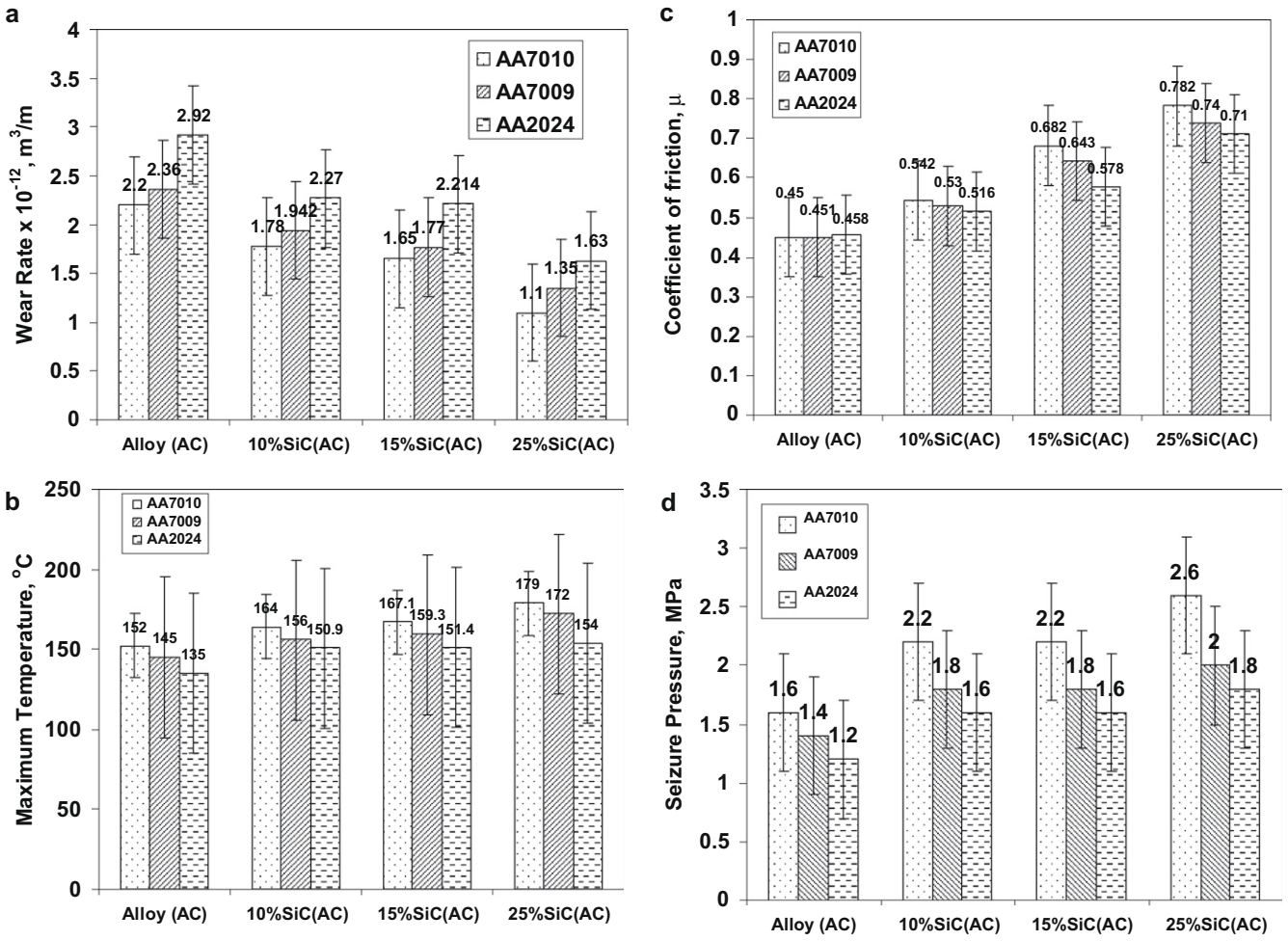

Fig. 3. Effect of matrix alloy on (a) wear rate; (b) maximum temperature; (c) coefficient of friction; (d) seizure pressure; sliding velocity: 3.35 m/s.

In the case of AA7010 alloy system, the seizure temperature for 10, 15 and 25 wt.% SiC reinforced composites are noted to be 164, 167.1 and 179 °C. In virgin alloy or in composites the seizure temperature is increased marginally by 14–16 °C due to change of matrix alloy from 2024 to 7010 alloy.

3.2.3. Effect of matrix alloy on coefficient of friction

The bar diagram represents that coefficient of friction for different alloy and their composites in as cast conditions at a sliding velocity of 3.35 m/s. It is evident from Fig. 3c that coefficient of friction does not follow any specific trend with matrix alloy. In case of virgin alloy the coefficient of friction is invariant to the alloy system. The coefficient of friction for 7010, 7009 and 2024 alloy are noted to be 0.45, 0.451 and 0.458 receptively. On the other hand, however in composite materials the coefficient of friction is noted to be marginally higher in 7010 alloy system as compared to the other alloy system. In 10 wt.% SiC composite, the coefficient of friction for 7010, 7009 and 2024 alloy system are noted to be 0.54, 0.53 and 0.516 respectively. In case of 25 wt.% SiC reinforced composites the coefficient of friction is noted to be higher as compared to that of 10 and 15 wt.% SiC reinforced composites. In these composites the coefficient of friction is noted to be highest for 7010 alloy system and least in 2024 alloy system. For example in case of 25 wt.% SiC reinforced composites the coefficient of friction for 7010, 7009 and 2024 alloy system are noted to be 0.78, 0.74 and 0.71 respectively. But SiC content significantly influence the coefficient of friction.

The change of alloy system leads to the variation of coefficient of friction by an average from 0.01 to 0.06, which is noted to be negligible. However, the coefficient of friction due to increase in SiC content from 0 to 25 wt.% is noted to be increased by an average from 0.33 to 0.35 depending on alloy system. Thus the coefficient of friction increases at an average rate of 0.123 per wt.% of SiC.

3.2.4. Effect of matrix alloy on seizure pressure

The bar diagram of seizure pressure of different alloy and composites at a fixed sliding velocity of 3.35 m/s is shown in Fig. 3d. It is evident form the figure that the seizure pressure varies with the alloy system; 7010 exhibited maximum seizure pressure, while 2024 exhibited minimum seizure pressure irrespective of processing condition and SiC content. In general, it is noted for all the alloy system that the seizure pressure for 10 and 15 wt.% SiC reinforced composites are almost same. However, 15 wt.% SiC reinforced composites travel for longer distance prior to seizure as was observed in Fig. 3d. For example, the seizure pressure of Al–15 wt.% SiC reinforced composite in as cast conditions for 7010, 7009 and 2024 alloy systems are 2.2, 1.8 and 1.6 MPa respectively. The seizure pressure of the composite increase significantly when SiC content increased from 15 to 25 wt.%, the seizure pressure for 25 wt.% SiC reinforced composite in as cast conditions for 7010, 7009 and 2024 alloy system are noted to be 2.6, 2.0 and 1.8 MPa respectively.

On an average in case of alloy the seizure pressure increases by 0.4 MPa, when the alloy changes from 2024 to 7010 alloy system.

In case of 10 and 15 wt.% SiC reinforced composite, this increment was noted to be 0.6 MPa, while incase of 25 wt.% SiC reinforced composite the increment of seizure pressure due to change of alloy system from 2024 to 7010 system is noted to be 0.8 MPa. The change of SiC content from 0 to 25 wt.% in case of 2024 alloy matrix, the seizure pressure increased by 0.6 MPa. While in case of 7010 alloy system due to change in SiC content from 0 to 25 wt.% leads to increase in seizure pressure by 1.0 MPa. This signifies that matrix alloy plays a dominant role in enhancing seizure pressure of composite system.

3.3. Worn surface of alloy and composites

Worn surface of aluminium alloy at an applied pressure of 0.6 MPa is shown in Fig. 4a. It indicates formation of continuous wear grooves (marked A) and relatively smoother MML and some damaged regions (Fig. 4a (arrow marked)). However, the degree of formation of cracks on the wear surface is not much. The worn surface of alloy at an applied pressure of 1.4 MPa, the wear surface is characterized by the formation of parallel lips (marked A) along the groove marking in Fig. 4b. The flow of materials along the sliding direction, generation of cavities due to delamination of surface material and tearing of surface material is also seen. The worn surface of composite, at an applied pressure of 0.6 MPa, is shown in Fig. 4c. It shows continuous grooves (marked A) and relatively smoother MML, patches of damaged regions (arrow marked). The worn surface of composite at seizure pressure of 2.0 MPa is shown (Fig. 4d), it also depicts material flow (marked A), cavities due to delamination of materials, flow of materials along sliding direction, tearing of material and surface cracks. It indicates greater degree of worn surface (flow of material in wavy form) and localized adhesion between specimen surface and counter body at the time of seizure.

3.4. Subsurface of alloy and composite

Fig. 5a, a higher magnification subsurface micrograph of aluminium alloy at an applied pressure of 0.6 MPa, clearly delineates highly deformed region. It depicts plastically deformed Al and void formation. During the sliding action, these voids joined together and formed wear debris, voids are arrow marked. Fig. 5b, a typical subsurface microstructure of aluminium alloy at an applied pressure of 1.0 MPa, the highly deformed region (MML) of the order of 20 μm (marked A) can be seen in this figure. The partial deformed region, which extended up to a distance of 40 μm (marked B) can be seen. This figure also clearly depicts the flow of Al dendrites (marked C) along the direction of sliding. A subsurface micrograph of composite Fig. 5c, at an applied pressure of 0.6 MPa, clearly shows highly deformed regions and SiC particle in the partially deformed region, the SiC particles are found intact in the subsurface region, there is not much effect of particle in the subsurface region even at higher load. A typical subsurface microstructure of composite at an applied pressure of 2.0 MPa (seized), it clearly shows SiC particle in highly deformed region. This clearly delineates that the SiC particles did not break even due to the high pressure.

Overall observation of subsurface of 7xxx-SiC composite states that the mode of deformation is more or less same irrespective of the concentration of SiC particle. In the case of high concentration of SiC particle the material seizes at higher load and in that case the SiC particle tends to crack. This did not observe in composite because the material seizes at low load condition. The other phenomenon such as voids formation and joining of voids are also prevailed in the case of composite material.

4. Discussion

It is noted that the overall alloying elements are higher in AA7010 alloy as compared to 7009 and 2024 alloy in Table 1. As a result, the amount of intermetallic precipitate is expected to be more in 7010 alloy as compared to 7009 and 2024 alloy. This results in the maximum hardness in 7010 alloy and minimum in 2024 alloy. Because of these facts the wear rate of 2024 alloy is noted to be maximum and the minimum wear rate is noted for 7010 alloy. The strength at room temperature as well as elevated

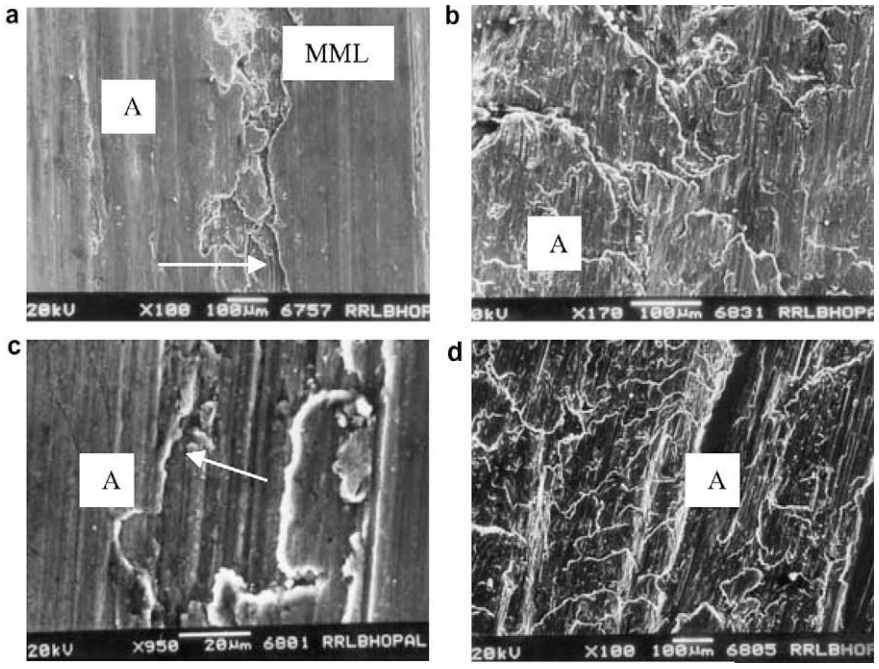

Fig. 4. A typical scanning electron micrograph of wear surface of (a) alloy at an applied pressure of 0.6 MPa, (b) alloy at seizure pressure, (c) composite at an applied pressure of 0.6 MPa, (d) composite at seizure pressure.

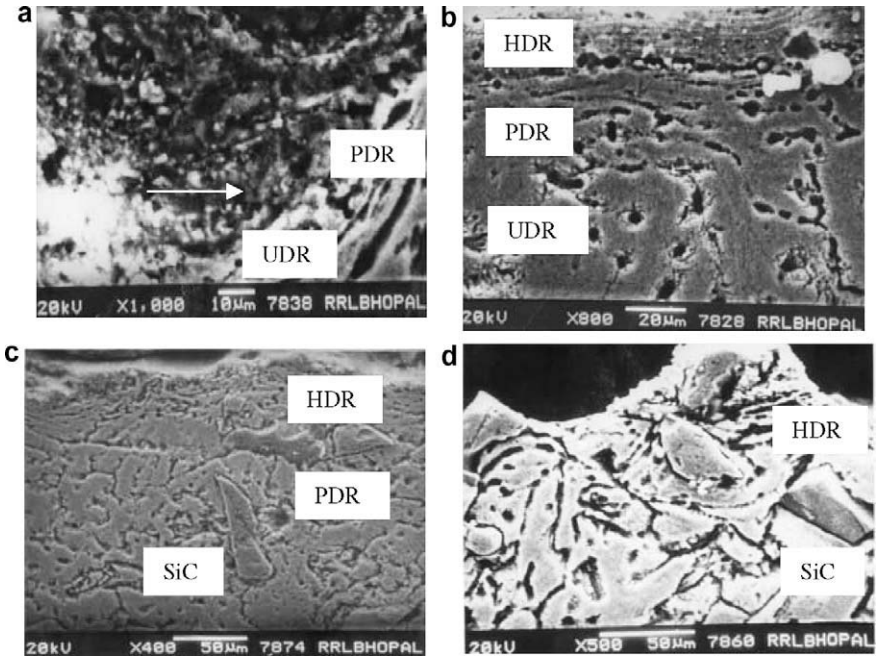

Fig. 5. A typical scanning electron micrograph of subsurface of (a) alloy at an applied pressure of 0.6 MPa, (b) alloy at an applied pressure of 1.0 MPa, (c) composite at an applied pressure of 0.6 MPa, (d) composite at seizure pressure (HDR – highly deformed region, PDR – partially deformed region, UDR – undeformed region).

temperature is noted to be more in 7010 alloy and 2024 alloy, the later one exhibited less strength at room temperature as well as at elevated temperature. Additionally the solidus and liquidus temperature of 7010 alloy is noted to be 615 and 650 °C, while those of 2024 and 7009 alloy are 500 and 340 °C and 600 and 640 °C respectively. The thermal conductivity and specific heat of 7010 alloy are 150 W/mK and 960 J/kg K, while those for 2024 alloy and 7009 alloy are 140 W/mK and 875 J/kg K and 150 W/mK and 875 J/kg K [18]. It is understood that during sliding considerable heat is generated and the extent of heating depends on strength, thermal conductivity and specific heat. Higher the strength less is the extent of heating [19]. However, the extent of heating decreases as the thermal conductivity and specific heat increases. Because of these facts, it is expected to have extent of heating in case of 2024 alloy and relatively less heating incase of 7010 alloy. As the solidus temperature of 7010 alloy is higher than the other two alloys, it can sustain more frictional heating and reduce the extent of localized adhesion due to partial fusion of surface material. As a result, 7010 alloy exhibited higher seizure temperature as well as higher seizure pressure. Due to the same reason 7009 alloy and composite exhibited higher seizure temperature and seizure pressure as compared to 2024 alloy and composite system. The coefficient of friction is primarily governed by the surface roughness and the experimental parameters. The surface roughness is almost invariant to the alloy system and thus at a given experimental parameters, the coefficient of friction is noted to be almost invariant to the alloy system (Fig. 3c).

A systematic approach to examine wear phenomena and transitions in wear mechanism over wide ranges of load and sliding speed was first adopted by Welsh [20] in studies of the sliding wear of mild steel. Alpas and Zhang [21] investigated wear mechanism map for Aluminum alloys using sliding wear equation for seizure and flash temperature close to T_m leads to transition from mild wear to severe wear. This observation was also experimentally verified. Several investigators also expressed the severity of the wear from the calculation of wear coefficient. An attempt has been made to analyze the results expressed by Archard's wear equation (1), the wear rate of a material is directly influence by external variables, such as load, sliding distance, and sliding velocity, wear rate evaluated using a wear equation based on the work of Archard [22] is given by

$$Q = KW/H \tag{1}$$

where Q is the volume removed from the surface by wear per unit sliding distance, H the indentation hardness of the softer surface, W the normal pressure applied between the surface and K the Archard's wear coefficient is dimensionless always less than unity. The value of K provides valuable means of comparing severity of different wear processes. For sliding wear of metals typical values of K for the mild wear of metals are 10^{-4}–10^{-6}, while K becomes 10^{-3}–10^{-2} for severe wear.

An attempt is also made the wear equation proposed by Lim and Ashby [23] for seizure, oxidation dominated wear, severe oxidational wear. Among all the equations proposed by Lim and Ashby, Eq. (2) of the seizure is given by

$$\overline{F} = 1/(1+\alpha_t\mu^2)^{1/2}[1T_b - T_o)/20T_m \ln 10^6/\beta\bar{v}] \tag{2}$$

where $\overline{F}$ is the normalized pressure, α_t is the heat distribution coefficient, μ is the coefficient of friction, T_b is the bulk temperature (°C), T_o is the initial temperature (°C), T_m is the melting temperature (°C), β is the dimensional parameter for bulk heating, and $\bar{v}$ is the sliding velocity (m/s).

It has been proposed by these investigators that the ranges of normalized wear rate or wear coefficient are for different wear mechanisms for mild and severe wear are 10^{-4}–10^{-6}, and 10^{-3}–10^{-2} respectively and these values are also good agreement with the calculated values in the present investigation. However, in the present study it was found that within the selected range of applied load and sliding speed, the investigated materials get seized and the normalized pressure $\overline{F}$ for seizure point comes to be almost 1, which is a good agreement with the theoretical value of $\overline{F}$. Thus there is a possibility of transition of different wear mechanism from one to the others within the selected applied load and sliding speed. The prevailing wear mechanism such as mild wear, severe wear and seizure were experimentally identified through microscopic observation, studies of worn surface and subsurface. In the

present study the wear coefficient of the order of 10^{-5} is considered as mild wear and 10^{-4} is severe wear, taking strong support from worn surfaces observation of SEM analysis.

In general the wear coefficient decreases with increase in applied load before the specimen gets seizes. This is because the surface is covered with more stable, smoother and harder MML, which leads to the generation of fewer wear particles, the rise in temperature also more at higher applied load, which makes the material more plastic. This is also one cause of the lower wear particles generation. Some of the particles that re generated during sliding may also become compacted and lead to a further decrease in *K*. the value of *K* decreases with increase in sliding speed before the material seizes. This is also because of the greater plasticity due to higher frictional heating and formation of a more stable MML over the specimen surface. At seizure, the MML becomes unstable and fresh material is exposed to the counter surface. Because of the high temperature, the freshly exposed material becomes fused in localized region and adheres to the counter surface, leading to the generation of more wear particles or the transfer of more softer Al alloy matrix to the counter surface. This leads to a higher valued of *K* during seizure.

As the SiC content increases, the degree of effective contact between the asperities of composite surface and counter surface decreases and thus the wear rate of composite reduces with increase in SiC content. The addition of SiC also improves the hardness, strength and Young's modulus of composite material as compared to the alloy. The high temperature strength, hardness and modulus of elasticity of composite also increase with increase SiC content. As a result, the sticking tendency due to softening of surface material with the counter surface reduces in case of composite as compared to the alloy. As a result, the seizure pressure of composite is noted to be significantly higher than that of the alloy. The MML, in composite, is thicker than that of alloy and it contains more amount of iron and Al oxide as compared to that in alloy. This makes the MML of composite stronger than that in alloy. Additionally, the MML in composite have the higher capability to withstand more frictional heating without localized adhesion. This is also one of the reasons to have higher seizure pressure and seizure temperature as compared to the alloy. This is exactly observed in all the alloys and composites investigated in the present study. Because of the lower degree of contact between the contact surfaces the temperature rise in case of composite is noted to be less as compared to the alloy. Additionally a large amount of energy is spent on scratching of counter surface by the SiC particles and thus less energy is spent on heating of the specimen surface. Further more, the thermal conductivity of the thicker MML formed over the composite surface is less as compared to that formed over alloy surface. The specific heat of MML in composite is also expected to be less as compared to that in alloy as the MML in composite contains more iron as compared to that in alloy. These facts lead to less temperature rise on composite surface as compared to the alloy. The thickness and concentration of MML, and the effective contact between the counter surfaces decreases with increase in SiC content which might be the prime factor for reduction in temperature rise with increase in SiC content.

It has been mentioned that the hard SiC particles penetrate deep into the counter surface leading to formation of microchips from counter surface. As a result grater amount of frictional force required for sliding of composite over the counter surface. Additionally the temperature rise is also noted to be less in composite as compared to the alloy. This leads to reduction in slipping action incase of composite as compared to the alloy. As a result coefficient of friction in case of composite is noted to be more than the alloy. As the SiC content increases number of SiC particles penetrating to the counter surface increases and thus the coefficient of friction in composites increases with increase in SiC content. The temperature rise is also noted to be decreased with increasing SiC content. Thus the slipping action is also reduced with increasing SiC content. This further leads to increase in coefficient of friction of composite with increase in SiC content (Fig. 3c).

5. Conclusions

From the experimental results the following conclusions can be drawn:

1. Sliding wear behaviour of the alloy and composites were studied as a function of reinforcement volume fraction, matrix alloy for all the three matrix alloy systems. Response parameters such as wear rate, seizure pressure, temperature rise and coefficient friction are measured during the tests.
2. The wear resistance of the alloy is improved significantly due to particle addition. The wear rate decreases with increase in SiC content irrespective of material. At initial period, the temperature rise in the alloy sample is noted to be minimum. Amongst the composite samples, temperature rise is noted to be maximum in Al–25 wt.% SiC composite and minimum in the case of Al–10 wt.% SiC reinforced composite.
3. 2024 alloy system suffers from highest wear rate, where as the 7010 alloy system exhibited least wear rate irrespective of SiC content and processing condition. Matrix alloy and SiC reinforcement play an important role in controlling the wear behaviour.
4. In a nut cell increase in seizure temperature due to change of SiC content from 0 to 25 wt.% is noted to be around 25 °C. Thus on an average seizure temperature increases at the rate of 1 °C/wt.% SiC.
5. The coefficient of friction increases at an average rate of 0.123 per wt.% of SiC.
6. Seizure pressure varies with the alloy system, 7010 exhibited maximum seizure pressure, while 2024 exhibited minimum seizure pressure irrespective of processing condition and SiC content.
7. The wear coefficient decreases with increasing applied pressure reaching to a minimum value and then again increases when the applied pressure reached near to the seizure of the specimen.
8. Reliability of sliding wear test procedure was examined by comparing the measured wear rate data with calculated wear rate by Archard equation at different loads and sliding speeds. It is noted that the measured values are in good agreement with the theoretically calculated value.
9. The maximum deviation of experimental values from the theoretical ones is noted to be around 10–15%. This supports the reliability of the test procedures and reproducibility of the test data. The reliability and reproducibility of tests were further supported through the comparison of measured normalized pressure $\overline{F}$ and theoretically calculated $\overline{F}$.
10. It is interesting to note that the seizure pressure of composites hardly affected when SiC content increase from 10 to 15 wt.%. This may be attributed to the fact that high temperature flowbility of the composite systems may not be changing when SiC content increased from 10 to 15 wt.%.
11. At lower applied pressures, formation of continuous grooves and some damaged regions observed on worn surfaces of the samples. Series of parallel transverse as well as longitudinal cracks and damaged regions were observed at higher applied pressures. Formation of parallel lips (wave like material flow) along the sliding direction observed at seizing of the sample.

12. Overall observation of subsurface of composite stated that the mode of deformation is more or less same irrespective of the concentration of SiC particle. The matrix flow is resisted by the particles and due to interaction of flow of matrix and SiC particles, the later one tends to rotate leading to matrix flow of more randomly in the surrounding area.

References

[1] Nussbaum AI. Light Metals. Age 1997;55(1&2):54.
[2] Rohatgi PK. Cast metal matrix composites metal hand book, 9th ed., vol. 15. ASM International; 1988.
[3] Sannino AP, Rack HJ. Dry sliding wear of discontinuously reinforced aluminium composites: review and discussion. Wear 1995;189:1–19;
Sannino AP, Rack HJ. Tribological investigator of 2009 Al–20 vol.% SiCp/17–4 PH, Part I: composite performance. Wear 1996;197:151–9.
[4] Sharma SC. The sliding wear behaviour of Al6061-garnet particulate composites. Wear 2001;249:1036–45.
[5] Jiang JQ, Tan RS, Ma AB. Dry sliding wear behaviour of Al_2O_3Al composites produced by centrifugal force infiltration. Mater Sci Technol 1996;12:483–8.
[6] How HC, Baker TN. Characterization of sliding friction-induced subsurface deformation of Saffil-reinforced AA6061 composites. Wear 1999;232:106–15.
[7] Venkataraman B, Sundararajan G. The sliding wear behaviour of Al–SiC particulate composites. II. The characterization of subsurface deformation and correlation with wear behaviour. Acta Metall Mater 1996;44:461–73.
[8] Wilson S, Alpas AT. Wear mechanism maps for metal matrix composites. Wear 1997;212:41–9.
[9] Mondal DP, Das S, Rao RN, Singh M. Effect of SiC addition and running-in-wear on the sliding wear behaviour of Al–Zn–Mg aluminium alloy. Mater Sci Eng 2005;A402:307–19.
[10] Rosenberger MR, Schvezov CE, Forlerer E. Wear of different aluminum matrix composites under conditions that generate a mechanically mixed layer. Wear 2005;259:590–601.
[11] Basavarajappa S, Mohan Chandra, Davim Paulo. Application of Taguchi Techniques to study dry sliding wear behaviour of metal matrix composites. Mater Des 2007;28:1393–8.
[12] Qin QD, Zhao YG, Zhou W. Dry sliding wear behavior of Mg_2 Si/Al composites against automobile friction material. Wear 2008;264:654–61.
[13] Mondal DP, Das S, Jah N. Drysliding wear behaviour of aluminium syntactic foam. Mater Des 2009;30:2563–8.
[14] Rao RN, Das S, Mondal DP, Dixit G. Dry sliding wear behaviour of cast high strength aluminium alloy (Al–Zn–Mg) and hard particle composites. Wear 2009;267:1688–95.
[15] Sahin Y, Murphy S. Wear performance of aluminium alloy composites containing unidirectionally oriented silicon carbide coated boron fibres. Wear 1996;197:248–54.
[16] Murphy S, Arikan R. A metallographic study of wear in planar random fibre-reinforced composites with an aluminium–zinc–copper alloy matrix. Wear 1992;155:105–15.
[17] Norman AF, Hyde K, Costello F, Thompson S, Birley S, Prangnell PB. Mater. Sci Eng A 2003;354:188.
[18] Davis JR. Aluminum and Aluminum Alloys. ASM Hand Book; 1998. p. 1-46.
[19] Sarkar AD. Wear of metals. International series on materials science and technology, vol. 18. Pergamon Press; 1976.
[20] Welsh NC. Philos Trans RoySoc Ser 1965;A257:51.
[21] Alpas AT, Zhang J. Wear regimes and transitions in Al_2 O_3 particulate reinforced aluminum alloys. Mater Sci Eng 1993;A161:273–84.
[22] Archard JF. J Appl Phys 1953;24:981–8.
[23] Lim SC, Ashby MF. Wear mechanism maps. Acta Metall 1987;35:1–24.